JOURNAL OF GUIDANCE, CONTROL, AND DYNAMICS
Vol. 19, No. 2, March–April 1996

Nonlinear Vibrations in the Tethered Satellite System-Mission 1

S. Bergamaschi,* P. Zanetti,† and C. Zottarel†
University of Padova, 35131 Padova, Italy

The theoretical and experimental dynamics of tethered satellite system-mission 1 in stationkeeping conditions are analyzed. For the mathematical part, a new model is presented that can take into account finite amplitudes of the satellite attitude motion. The analysis of the data of the accelerometric package onboard is carried out with a method insensitive to the blanks frequently present in the data flow. The spectral frequencies are compared with the results of the model and both of the uncertainties are evaluated. Finally, the physical causes that produce several peaks in different frequency ranges from 10^{-3} to 1 Hz are discussed.

Nomenclature

A	= tether cross section
D_1	= $\partial()/\partial(T_1)$
D_0	= $\partial()/\partial(T_0)$
d	= distance from satellite center of mass to tether attachment point
E	= Young's modulus of tether material
g	= gravity acceleration
I	= roll (or pitch) moment of inertia
l	= tether length (constant)
m	= satellite mass
n	= mean motion of reference orbit
s	= space variable along the tether
T	= tether tension at the satellite in equilibrium conditions
T_i	= $\varepsilon^i t$, slow times
t	= time variable
(X, Y, Z)	= reference system used to define the orientation of the satellite linear accelerometer sensitive axes; Y toward the orbit pole and Z parallel to the upward local vertical
$x(l, t)$	= longitudinal displacement of the terminal (at the satellite) tether section
(x, y, z)	= reference system centered at the Shuttle end of the tether, with x parallel to the ascending local vertical and z toward the orbit pole; used to derive the equations of motion
$y(l, t)$	= transverse, either in-plane or out of plane, displacement of the terminal tether section
β	= nondimensional wave number of longitudinal vibrations
ε	= small ordering parameter
$\vartheta(t)$	= satellite roll (or pitch) angle
λ	= nondimensional wave number of transverse vibrations
μ	= tether mass per unit length
$'$	= space derivative
$\cdot$	= time derivative

I. Introduction

THEORETICAL and experimental investigation on tethered satellite system-mission 1 (TSS-1) dynamics is a research program to study the dynamics of TSS-1, flown in August 1992. After the mission, the data from the pertinent instruments (accelerometers, gyros, and tensiometer) are being compared with the expectations of mathematical models already implemented; the first results have been presented to the scientific community.[1,2] Some conclusions, among others, are as follows:

1) The experimental and theoretical values of the frequencies of satellite roll-pitch and of the low-order modes of tether transverse vibrations are in good agreement.

2) The satellite linear accelerometer (SLA) is also sensitive enough to detect the lower modes of the structural vibrations of the deployer boom and of the orbiter.

3) Quite frequently the spectra exhibit more spikes than expected by a linear modal analysis.

4) The most important error source is the lack of resolution in the spectral analysis.

The work instruments used were the fast Fourier transform (FFT) and maximum entropy method for the data analysis in the frequency domain and a numerical–analytical model based on the assumption of small amplitude vibrations. The spectra obtained and the model adopted in Ref. 1 have been very useful to characterize the most important components of the acceleration field at the satellite, but some limitations have precluded a more detailed dynamics investigation. The most stringent constraint of the experimental analysis has been the presence of several blank time periods in the data flow that have ruled out the possibility of detecting the very slow tether librations and have considerably reduced the accuracy of the estimation of the harmonic components with periods comparable to 100 s, because of relatively poor resolution of the FFT at low frequencies. On the theoretical side, the most restrictive assumption seems to have been the one related to the vibration amplitudes. In fact, it has already been mentioned that the spectra are denser than expected. Although some of the additional peaks can be attributed to structural vibrations of the whole system in space or to controlled motions [e.g., satellite yaw, or orbiter attitude and orbit control system (AOCS) firings], the frequencies of others appear to be linear superpositions of some fundamentals predicted by the linear model. The action of nonlinear couplings has, therefore, been suggested to explain the presence of such combination tones; this possibility has been confirmed by numerical simulations.[2]

The present work considers the SLA data and attempts to improve the accuracy of the estimates done so far, by using both a more sophisticated method for data analysis and a mathematical model that takes into account one of the possible nonlinearities of the system.

The blanks problem has been considerably alleviated by using the Lomb periodogram,[3] which accepts input data unevenly distributed in time. The nonlinearity included in the new model is the one originated by the finite amplitude of satellite pitch and roll.

II. Mathematical Model

The model to follow is an extension of the linear one presented in Ref. 1, and so the major assumptions are not repeated for the sake of brevity. It is only noted that for most of the mission time the satellite was in hold mode, i.e., its yaw motion was controlled actively, so

Presented as Paper 94-3735 at the AIAA/AAS Astrodynamics Conference, Scottsdale, AZ, Aug. 1–3, 1994; received Nov. 7, 1994; revision received Oct. 26, 1995; accepted for publication Oct. 30, 1995.

*Associate Professor and Theoretical and Experimental Investigation on TSS-1 Dynamics Principal Investigator, Department of Mechanical Engineering. Member AIAA.

†Research Assistant, Department of Mechanical Engineering.

that excursions larger than 1 deg from the reference attitude were prevented. This entails that since tether in-plane elastic vibrations (not the librations) are almost coincident with out-of-plane vibratory motions, the dynamics can be considered two dimensional if the purpose is to study tether elastic modes, satellite attitude frequencies, and combinations thereof. The generalization inherent in this model seemed necessary to the authors after a careful examination of the SLA spectra obtained previously, which suggested that nonlinear terms should be taken into account in the dynamical equations. Such terms might be the result of physical causes, tether nonlinear elastic behavior, or geometrical factors, small but finite amplitudes, of both tether vibrations and satellite oscillations. In turn, the physical causes just mentioned may be different and include tether memory of physical environment, stress, shape before the mission, in relation to a very small equilibrium tension during the mission, and complex structure and material composition, causing tether EA to depend sensibly on tension and, therefore, equilibrium length and in-line thrusters operations.

Turning to the geometrical characteristics of the motion, note that during most of the stationkeeping periods the tether vibrations have not violated the small-amplitude assumption (a maximum sag of a few meters is still small, in comparison with a length of some 200 m), whereas satellite roll-pitch have several times reached amplitudes larger than 0.1 rad. Therefore, because of lack of information about tether material behavior and also the complexity of the related models, the nonlinearity simulated in this model is the one caused by satellite attitude dynamics.

A source of confusion must be mentioned at this point. The reference system for the mathematical model is the one with x along the ascending local vertical and z parallel to the orbit pole; it is adopted here in coherence with the formalism of other papers on the same subject, written several years before the mission. Unfortunately, the reference system adopted, after the mission, to characterize the data of all of the scientific instruments has X in the direction of the (circular) orbital velocity and Z along the ascending local vertical. Thus, in the following, capital letters will be used for the experimental axes.

Using the same method adopted in Ref. 1, the equations of motion can be written as

$$\begin{aligned}
&\ddot{x} - d\ddot{\vartheta}\sin\vartheta - d\dot{\vartheta}^2\cos\vartheta + (EA/m)x' = 0\\
&\ddot{y} + d\ddot{\vartheta}\cos\vartheta - d\dot{\vartheta}^2\sin\vartheta + 3n^2(l + d\cos\vartheta)y' = 0\\
&\ddot{\vartheta} + K_1(\ddot{y}\cos\vartheta - \ddot{x}\sin\vartheta) + K_2(l + x + d\cos\vartheta)\sin\vartheta = 0
\end{aligned} \tag{1}$$

where

$$K_1 = md/(I + md^2) \qquad K_2 = 3mn^2d/(I + md^2)$$

It is easily seen that, in the linear approximation, longitudinal tether vibrations are not coupled to transverse oscillations and satellite roll/pitch. Equations (1) may be considered to be the generalization (for non-infinitely small ϑ) of the linear differential system in Ref. 1, where the assumptions and limitations of the model are discussed in some detail. The discussion is not repeated here for the sake of brevity.

The method of multiple scales has been used to solve system (1) where x and y are assumed to be first-order infinitesimals, and $\sin\vartheta$ and $\cos\vartheta$ are expanded in series. If ε is a small parameter, the solution of Eqs. (1), to the third order of ε, has the form

$$\begin{aligned}
x(s,t,\varepsilon) &= \varepsilon x_1(s, T_0, T_1, T_2) + \varepsilon^2 x_2(s, T_0, T_1, T_2)\\
&\quad + \varepsilon^3 x_3(s, T_0, T_1, T_2)\\
y(s,t,\varepsilon) &= \varepsilon y_1(s, T_0, T_1, T_2) + \varepsilon^2 y_2(s, T_0, T_1, T_2)\\
&\quad + \varepsilon^3 y_3(s, T_0, T_1, T_2)\\
\vartheta(t,\varepsilon) &= \varepsilon\vartheta_1(T_0, T_1, T_2) + \varepsilon^2\vartheta_2(s, T_0, T_1, T_2)\\
&\quad + \varepsilon^3\vartheta_3(s, T_0, T_1, T_2)
\end{aligned} \tag{2}$$

where $T_0 = t$ and T_1 and T_2 are the slow times $T_i = \varepsilon^i \cdot t$. Substituting Eqs. (2) in Eqs. (1) and equating separately to zero the terms of different order in ε, three systems of equations are obtained. The first-order system is identical to the one presented in Ref. 1, so that, after variable separation, its solution at the satellite end of the tether is

$$\begin{aligned}
x_1(l,t) &= \left[A_1\exp(i\omega_1 T_0) + A_1^*\exp(-i\omega_1 T_0)\right]\sin\beta\\
y_1(l,t) &= \left[A_2\exp(i\omega_2 T_0) + A_2^*\exp(-i\omega_2 T_0)\right]\sin\lambda\\
\vartheta_1(t) &= A_3\exp(i\omega_2 T_0) + A_3^*\exp(-i\omega_2 T_0)
\end{aligned} \tag{3}$$

where the asterisks indicate complex conjugations, $A_i = A_i(T_1, T_2)$, and ω_1 and ω_2 are the frequencies of each vibration mode of the x and $y-\vartheta$ vibrations, respectively. A second index for the mode order is not used here for simplicity of notation. Further, β is the generic solution of the frequency equation

$$\beta\cdot\tan\beta = \mu l/m; \qquad \omega_1 = (\beta/l)\sqrt{EA/\mu} \tag{4}$$

and λ is a solution of

$$\lambda\tan\lambda = \frac{\mu l}{m}\left(1 + \frac{md^2\lambda^2}{I\lambda^2 - \mu d l^2}\right); \qquad \omega_2 = \frac{\lambda}{l}\sqrt{\frac{T}{\mu}} \tag{5}$$

The second-order system is

$$\begin{aligned}
&D_0^2 x_2 + (EA/m)x_2' = d(D_0\vartheta_1)^2 + d\vartheta_1\left(D_0^2\vartheta_1\right) - 2D_0D_1x_1\\
&D_0^2 y_2 + d\left(D_0^2\vartheta_2\right) + 3n^2(l+d)y_2' = -2D_0D_1y_1 - 2d(D_0D_1\vartheta_1)\\
&D_0^2\vartheta_2 + K_1\left(D_0^2 y_2\right) + K_2(l+d)\vartheta_2 = -2D_0D_1\vartheta_1\\
&\quad - 2K_1(D_0D_1y_1) + K_1\vartheta_1\left(D_0^2x_1\right) - K_2x_1\vartheta_1
\end{aligned} \tag{6}$$

After elimination of the secular terms, its solution has the form

$$\begin{aligned}
x_2(l,t) &= B_1e^{2i\omega_2T_0} + B_1^*e^{-2i\omega_2T_0}\\
y_2(l,t) &= C_1e^{i\Omega_1T_0} + C_2e^{-i\Omega_1T_0} + C_3e^{i\Omega_2T_0} + C_4e^{-i\Omega_2T_0}\\
\vartheta_2(t) &= D_1e^{i\Omega_1T_0} + D_2e^{-i\Omega_1T_0} + D_3e^{i\Omega_2T_0} + D_4e^{-i\Omega_2T_0}
\end{aligned} \tag{7}$$

where $\Omega_1 = \omega_1 + \omega_2$, $\Omega_2 = \omega_1 - \omega_2$, and B_i, C_i, and D_i are cumbersome constants to be found after some algebra. The explicit form of some of them can be found in the Appendix.

From Eqs. (7) it is seen that longitudinal vibrations are forced by the other degrees of freedom, whereas combination tones appear in the $y-\vartheta$ motion with frequencies equal to the sum, or difference, of the frequency of the ith longitudinal mode and the one of the jth transverse-attitude mode.

The third-order formulas are not shown because, as can easily be suspected, they are excessively long. In any case, the characteristics of the final solution are already apparent in Eqs. (7). In summary, they are as follows.

1) For reasonable amplitude, the frequencies of the nonlinear modes differ only slightly from the corresponding values of the linear problem. Thus, Eqs. (4) and (5) can be used with negligible errors for frequency computations

2) The number of combination frequencies is considerably increased with respect to the second-order solution (see Appendix).

3) Small denominators may characterize some amplitudes, depending on near commensurabilities between some fundamental modes. An example is Eq. (A1) in the Appendix.

The last step of the model is the computation of the acceleration field at the SLA, which implies the calculation of the second time derivative of the radius vector from the Shuttle end of the tether to the SLA position inside the satellite and the application of the rotation matrix (to the third order in the attitude angles) between the principal inertia system of the satellite and the orbital reference frame.

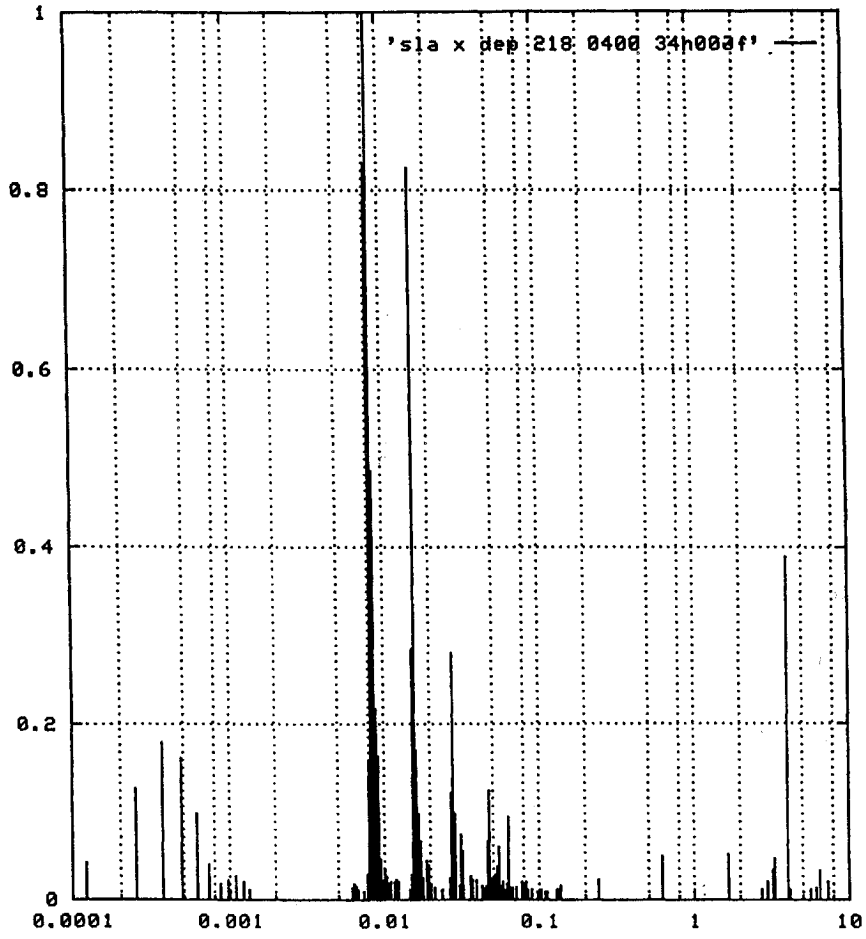

Fig. 1 SLA-X power spectral density (PSD) in a relative quiet period during stationkeeping at 256 m.

Again, the resulting formulas cannot be written extensively. To give an idea of the possible combinations, however, let us consider the acceleration on SLA-Y and carry out the computation steps to the third order in the angles. If ω_1 is the frequency of the spring-mass mode, $\omega_{2,n}$ is the frequency of the nth mode of the coupled $y-\vartheta$ problem, and ω_3 is the controlled yaw frequency (sensed by the SLA), then the following acceleration frequencies may be present in the Y spectrum:

$$\omega_{2,n};\quad 2\omega_{2,n};\quad 3\omega_{2,n};\quad \omega_3;\quad 2\omega_3;\quad 3\omega_3$$

$$\omega_1 \pm \omega_{2,n};\quad \omega_{2,n} \pm \omega_{2,m}(n \neq m);\quad \omega_3 \pm \omega_{2,n}$$

$$\omega_3 \pm 2\omega_{2,n};\quad \omega_{2,n} \pm 2\omega_3;\quad \omega_{2,n} \pm 2\omega_{2,m}(n \neq m)$$

$$\omega_3 \pm \omega_{2,n} \pm \omega_{2,m}(n \neq m)$$

It has been taken into account in writing these frequencies that the upper modes of longitudinal vibrations are outside the frequency band detectable by the SLA. Otherwise, a second index would also have been necessary for ω_1.

III. Data Analysis

The preliminary analysis of instruments performance, calibration procedure, and data characteristics have been discussed in Refs. 4 and 5 and summarized in Ref. 1. It is mentioned again that formerly the blanks problem precluded the possibility of a straightforward FFT of SLA data slices longer than 900 s (in the most favorable case). Therefore, a method capable to handle data unevenly distributed in time was needed and, after some search, subroutine FASPER in Ref. 3 was used, because remarkable features of the Lomb periodogram (implemented by the subroutine) are as follows: 1) the existence of a fast algorithm, particularly useful when more than 10,000 data may be processed at the same time; 2) contrary to the conventional FFT, the sampling frequency can be selected a priori (within certain margins); and 3) the possible evaluation of the significance level of each peak in the spectrum. The first use of the periodogram has been to evaluate the bias and bias time dependence of the instruments as accurately as possible. The procedure was rather elaborate and time consuming, so that it is reported only in extreme synthesis, because more detail can be found in Refs. 4 and 5; its main steps included the preliminary evaluation of the conditions and of the accuracy with which the Parseval theorem is satisfied by FASPER and the implementation of an inverse Lomb periodogram.[6] The logic is as follows. First is data acquisition and rejection/validation. Next is resampling at 2 Hz (16 Hz is the instruments sampling frequency). Since instrumental bias was expected to affect low signal frequencies, the rejection of valuable data has been necessary to reduce the data to a manageable number.

Filtering follows, to eliminate random peaks with low significance level. To be more specific, since the Lomb periodogram allows the evaluation of the significance level of any spike,[3] peaks with a less than 10^{-3} probability of being, because of the real signal, have been rejected. Last is the evaluation of the coefficients of the inverse algorithm and determination of the bias model order for each instrument.

The results can be summarized as follows.

For SLA-X, the bias is constant and equal to -0.187 mg. Its effect on harmonic components over 10^{-3} Hz is negligible with respect to other error sources.

For SLA-Y, the time dependence of the bias can be modeled with a cubic, the constant term of which is 0.890 mg, i.e., close to the value previously found in Ref. 4. Also in this case, it can affect frequencies lower than 10^{-3} Hz.

For SLA-Z, the performance of this sensor was known in advance to be anomalous because of an intermittent contact in the associated electronics. The analysis performed confirmed the wild behavior of the instrument, so that only the bias average during the three on orbit calibrations is given here, i.e., 3.378 mg. From the evaluation of the signal-to-noise ratio in different frequency ranges it is concluded

that harmonic components above 10^{-2} Hz are not sensibly affected by the bias. Of course, SLA-Z spectra have been considered with particular caution and assumed to be physically significant only after comparison with other instruments data, or theoretical results.

The fact that harmonic components with periods shorter than about 1000 s along the X and Y axes and shorter than 100 s along Z are free from bias errors is rather fortunate because it is known that if $l = 256$ m the longest fundamental periods (satellite roll/pitch) are just close to 100 s and are sensed directly by SLA-X and SLA-Y, whereas the most important fundamental mode in the vertical direction is the spring-mass mode, the period of which is expected to be close to 15 s.

In conclusion, the following four points describe the procedure used to obtain the spectra that will follow.

First is acquisition of the longest possible string of data from each instrument in stationkeeping conditions. To be more specific, the longest time intervals (routine case) have been 34 min because of memory (not time) problems in the computer. Next is data rejection/validation according to the criteria reported in Ref. 4. On the average, 3% of the data was discarded at the end of this process. Subroutine FASPER with OFAC = 4 and HIFAC = 1 is used. The use and meaning of these two parameters can be found in Ref. 3; their numerical values have been decided after several runs with different sets of data, both synthetically generated and real. Last is filtering and cancellation from the spectra of the peaks that according to the null hypothesis imbedded in the subroutine have a significance level equal to or less than 10^{-3}.

IV. Results

The first purpose of this paper was to confirm and extend the analysis on linear modes published in Ref. 1. Computed and measured periods values, as well as their associated errors, are shown in Table 1. The theoretical errors have been obtained by differentiating the pertinent frequency equations and assuming that some parameters, such as the mean motion and the tether length, are known exactly, so that the sources of uncertainty are the values of m (and, therefore, I) that decreased faster than expected during the mission from 518 to 481 kg; μ that was measured on the ground and changed slightly before the mission, probably in dependence of the different tether specimens being analyzed; and EA that has been reported in a Martin Marietta memo[7] to be critically dependent on tether tension. The value given next is computed from the experimental formula in the memo, i.e., $EA = 24{,}802.18T^{1/4}$, whereas the 10% error is arbitrarily (perhaps conservatively) adopted, to have a feeling of the frequency dependence on tether elastic characteristics. Note that although EA is a function of tether tension (or length), it is still meaningful to consider it constant, as has been done in Eqs. (1) if stationkeeping conditions are taken into account.

Table 1 Comparison between theoretical and experimental periods

Mode	Computed period, s	Measured period, s
Yaw (controlled)	300.1 ± 10.0	291.5 ± 5.2
Pitch	114.8 ± 3.7	114.0 ± 0.8
Roll	106.0 ± 3.4	107.5 ± 0.7
$T_{2,3}$	64.4 ± 2.1	63.6 ± 0.3
$T_{2,4}$	32.2 ± 1.0	32.0 ± 0.1
$T_{2,5}$	21.5 ± 0.7	21.3 ± 0.1
$T_{2,6}$	16.1 ± 0.5	16.2 ± 0.1
L_1	15.5 ± 0.8	15.6 ± 0.1
$T_{2,7}$	12.9 ± 0.4	12.9 ± 0.1

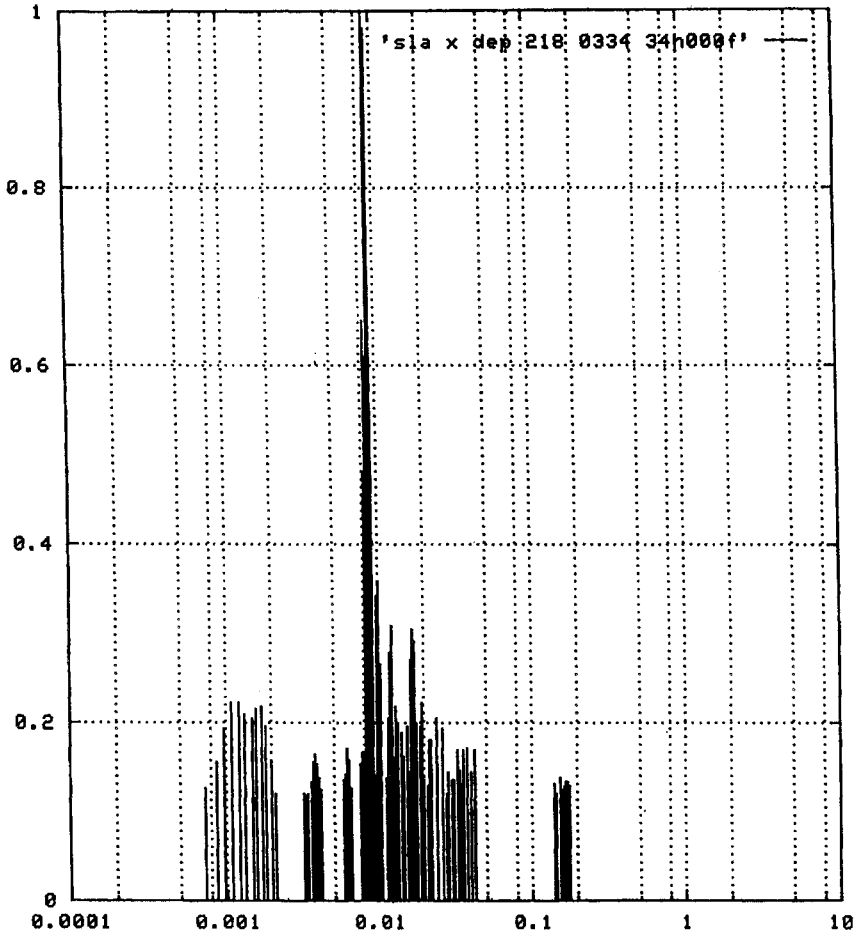

Fig. 2 SLA-X PSD with 34 min of data during stationkeeping at 256 m.

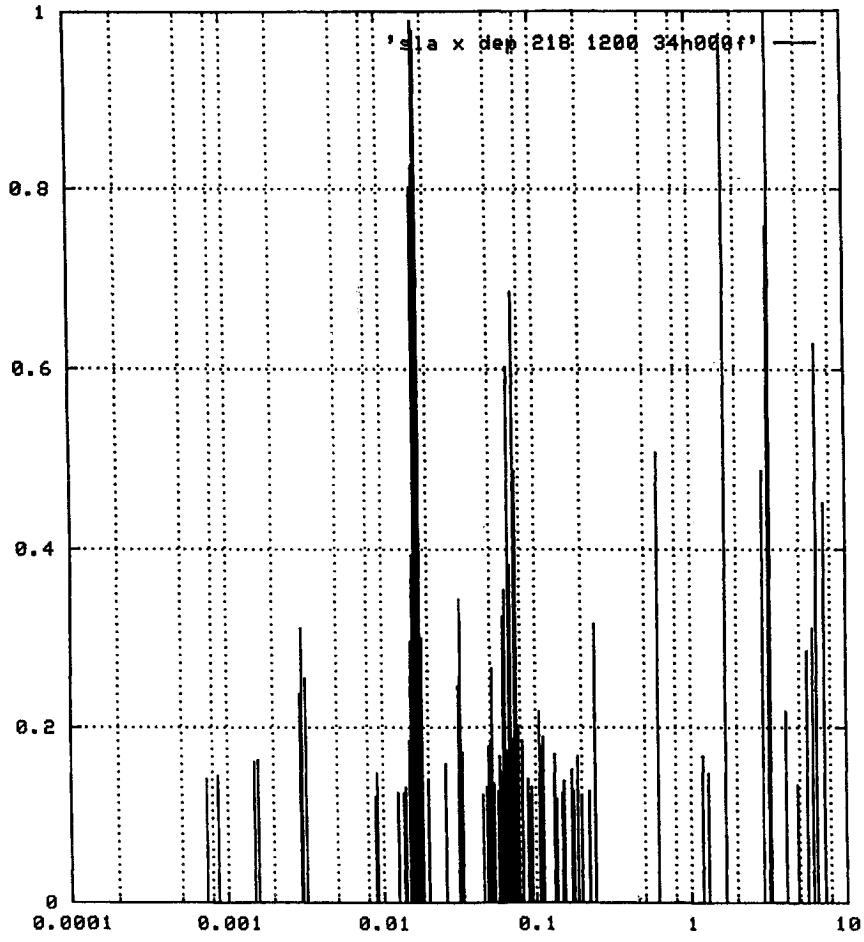

Fig. 3 SLA-X PSD in a noisy time interval at the end of the stationkeeping at 256 m.

Thus, the values in the formulas are

$$n = 1.158 \times 10^{-3}\,\text{rad/s} \qquad l = 256\,\text{m} \qquad I_r = 110\,\text{kg}\cdot\text{m}^2$$

$$I_p = 130\,\text{kg}\cdot\text{m}^2 \qquad m = 500 \pm 20\,\text{kg}$$

$$\mu = (8.2 \pm 0.2) \times 10^{-3}\,\text{kg/m} \qquad EA = 21025 \pm 2100\,\text{N}$$

The experimental errors caused by the finite duration of the data samples have been computed according to $|\Delta T| = T^2/8T_0$, where, in this formula, T is the period of the harmonic analyzed and T_0 the sample duration. The formula takes into account the oversampling factor OFAC.

In Table 1, $T_{2,j}$ is the period of the jth mode of coupled attitude/transverse vibrations; its theoretical value is computed from Eq. (5). The second subscript starts from 3 because the first root of the equation is the frequency of the in-plane libration (lower than the fundamental frequency) and the second is roll, or pitch, depending on the I value. Further, L_1 is the fundamental period of longitudinal vibrations (spring-mass). In the case of yaw, the theoretical value is simply the 1-h average of the periods measured by the yaw gyro during a time interval when the satellite was quiet and in hold mode. The experimental values have been obtained analyzing in succession all of the SLA-X and SLA-Y data during the stationkeeping at 256 m and averaging the results when (most usual case, in particular for low-order modes) well-defined peaks corresponding to the same mode appeared in more than one spectrum. The measured values are the ones corresponding to the frequency where each spike reached its maximum height; in this respect, it is noted that, since many spectra have been produced in the course of the analysis, only sharp peaks have been taken into account in the averaging process. This is why higher-order transverse modes have not been included in Table 1. The measured $T_{2,7}$ is the average of three peaks in different spectra with periods differing less than the measure uncertainty from each other. No such averaging was possible for $T_{2,8}$ or upper modes, even if peaks with periods matching the theoretical value were present in some spectra.

It is seen from Table 1 that the agreement between theory and data is good and that the errors are reasonably small, in particular on the experimental side; this is because of the very large number of data (more than 30,000) used to construct each spectrum and to the high sampling frequency of the instruments (16 Hz). The result for longitudinal vibrations, however, must be considered with care for a number of different reasons: the anomalous behavior of SLA-Z; the dependence of EA on tether tension, critical in particular if T is low, and lack of information on related uncertainty; the impossibility to detect upper modes because their frequencies are too high; and the position in the spectrum of L_1. It is seen in Fig. 4 that the SLA-Z spectral interval around 15 s is densely populated, so that, usually, several peaks are present with comparable heights. In any case, the value given in Table 1 is the average from two spectra with dominant peaks having frequencies differing less than the maximum uncertainty.

Some experimental results are shown in Figs. 1–4, where the frequencies are measured in hertz and the amplitudes have first been normalized with respect to the variance of the data and next scaled to the highest peak. Figure 1 is the X spectrum obtained during a quiet period (few thrusters disturbances). The spikes on the left, between 10^{-4} and 10^{-3} Hz, have little physical meaning because they correspond to the fundamental frequency (1.22×10^{-4} Hz) and to its lower multiples, perhaps modulated by the tether libration. The most important spikes are in the range 0.01–0.1 Hz; the highest two being originated by $\omega_{2,2} - n$ (pitch minus mean motion) and by $\omega_{2,3}$ (semisinusoidal transverse mode), respectively.

The right-hand part of the spectrum is almost tether independent. It has already been shown in Ref. 1 that most of the high-frequency lines can be attributed to deployer boom and orbiter vibrations. In

particular, the high peak at 4 Hz is close to the value expected by finite elements analysis for the frequency of the sixth structural mode of the boom.

Figures 2 and 3 show different, and to some extent complementary, phases of the stationkeeping at 256 m. In Fig. 2 the high-frequency components do not reach appreciable amplitudes, whereas the interval 10^{-3}–10^{-2} Hz is thickly populated. From the analysis of orbiter gyros it could be concluded that most of the lines between 1000 and 500 s are because of frequencies of the orbiter AOCS, whereas the peaks around 300 s are generated by satellite yaw control. The origin of the well-separated spectral contribution around 6–7 s is not yet clear. The same comment applies to a peak around 14 s, not visible in Fig. 2, but frequently present in other spectra.

The high-frequency components are dominant in Fig. 3. This feature is the result of several repeated short duration pulses of the satellite in-line thrusters that were fired in the attempt to change the tether length and excited structural vibrations. Some of the frequencies are in good agreement with the boom structural analysis, whereas others have no theoretical counterpart; in particular, the one at 1.6 Hz is present in several spectra and may be the result of the base structure of the boom.

The Y-axis spectra are not shown because their characteristics are not qualitatively different from those of SLA-X. A typical SLA-Z spectrum is shown in Fig. 4. This spectrum is typical in the sense that, in several cases, the most important contributions along Z are in the range 0.02–0.1 Hz.

Another purpose of the paper was the investigation of the contribution of combination tones to the spectral lines. It appears that several of them are present in some spectra of all of the instruments, their frequencies matching the theoretical values within the errors. This is also the case of the figures. In Fig. 2, three medium height peaks have the frequencies shown in Table 2. All are predicted by the theory, and the one with $T = 61.1$ s is quite frequent, being present and clearly discernible in at least nine different spectra; in fact, it is the second highest in Fig. 3.

Moreover, it is seen that the spike at 38.3 s appears also in Fig. 4, i.e., in a SLA-Z spectrum; further, $2\omega_{2,2}$, which is present in Fig. 3, is one of the most frequent (in 13 spectra). The appearance of

Table 2 Combination frequencies in the spectrum of Fig. 2

Mode composition	Period, s	Presences in different spectra
$\omega_3 + \omega_{2,2}$	83.1	2
$\omega_1 - \omega_{2,5}$	61.1	9
$3\omega_{2,2}$	38.3	2

Table 3 Measured and computed periods of the most important spikes in Fig. 5

Measured period, s	Computed period, s	Mode
1028 ± 220	1045 ± 23.00	$3T_1$
130.83 ± 3.57	125.47 ± 2.79	$T_{2,2}$
55.35 ± 0.64	55.40 ± 1.23	$L_1 - T_{2,5}$
27.68 ± 0.16	27.33 ± 0.60	$L_1 - T_{2,4}$
26.36 ± 0.16	26.95 ± 0.60	$T_{2,4}$
13.92 ± 0.04	13.63 ± 0.30	$L_1 - T_{2,1}$
13.58 ±0.04	13.57 ± 1.63	L_1
13.48 ± 0.04	13.51 ± 0.30	$L_1 - T_{2,1}$
13.38 ± 0.04	13.63 ± 0.30	$L_1 - T_{2,1}$
13.25 ± 0.04		
12.45 ± 0.03	12.24 ± 0.27	$L_1 + T_{2,2}$
9.14 ± 0.02	9.02 ± 0.20	$L_1 + T_{2,4}$

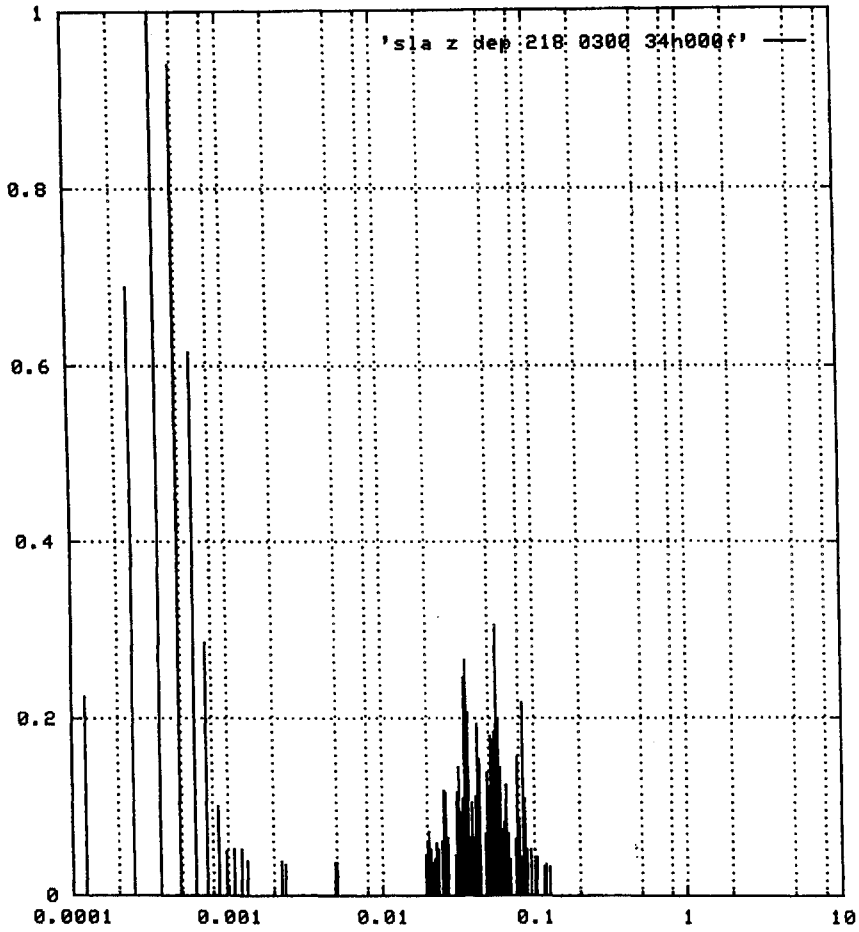

Fig. 4 Typical SLA-Z PSD; $l = 256$ m.

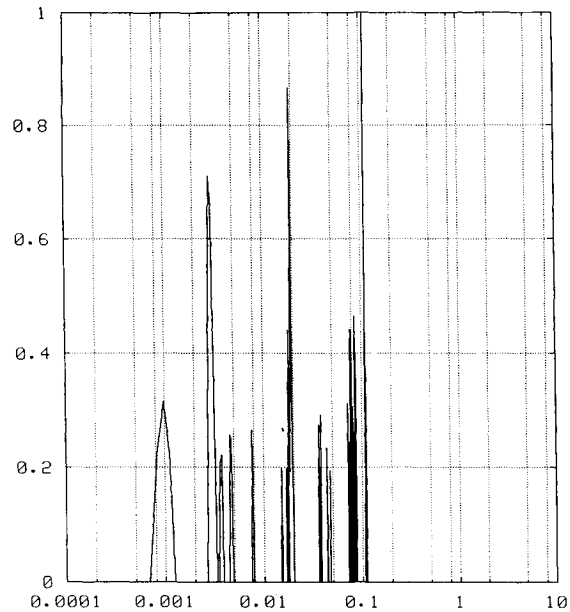

Fig. 5 SLA-Z PSD with several combination tones generated by the spring-mass mode; l = 179 m.

combination tones with ω_1 is interesting and important to establish that the period of the spring-mass mode at 256 m is really close to 15.5 s, so that the EA value and its dependence from tether tension are correct. This is confirmed by Fig. 5 and Table 3. Figure 5 is the spectrum of more than 28,000 SLA-Z data, in stationkeeping conditions at l = 179 m. Several spikes resulting from the combination of the spring mass with other modes are clearly discernible in this peculiar spectrum. Table 3 allows the comparison between computed and measured periods. The table notation is the same as in Table 1. Note that the numerical values are different from the ones already reported because of different tether length, tension, and EA. In any case, from the large number of combination tones both observed and predicted by the theory in the Z direction, it can be concluded that the spring-mass mode has been identified and that the model for EA is reasonable.

V. Conclusions

Many combination tones are visible in at least one spectrum, in accordance with the theory. On the other hand, however, a few low-order ones have never been detected. For instance, this is the case of $\omega_3 - \omega_{2,3}$. On the contrary, some spikes with remarkable amplitudes cannot be explained by this theory (or by other physical causes guessed so far); one such case, with period close to 6–7 s, has already been mentioned and is visible in Fig. 2.

Appendix: Some Formulas

Equations (7) show that the second-order solution of system (1) depends on the three sets of constants B_i, C_i, and D_i. Some of them, i.e., B_1, C_1, and D_1, are written here to give an idea of their structure and of some peculiar characteristics:

$$B_1 = -\frac{2d\alpha\omega_2^2}{(EA/ml)\,\beta^2 - 4\alpha\omega_2^2}A_3^2 = -\frac{2d\omega_2^2}{\omega_1^2 - 4\omega_2^2}A_3^2 \qquad \text{(A1)}$$

where

$$K_1 = \frac{md}{I + md^2} \qquad K_2 = \frac{3mn^2d}{I + md^2}$$

$$S_1 = -\left(K_1\omega_1^2 + K_2\right)\sin\beta A_1 A_3$$

$$S_1^* = -\left(K_1\omega_1^2 + K_2\right)\sin\beta A_1 A_3^* \qquad \Omega_1 = \omega_1 + \omega_2$$

and where α is the mass ratio ($\mu l/m$); the nondimensional frequency β is a generic eigenvalue [Eq. (4)] of the problem of longitudinal tether vibrations; the nondimensional frequency λ is an eigenvalue of Eq. (5), i.e., of the frequency equation for transverse tether vibrations coupled to satellite roll/pitch; A1 and A3 are the complex constants [Eqs. (3)] in the first-order solution, to be determined to satisfy the initial conditions; and the asterisk indicates complex conjugation.

The first peculiarity of the solution is the existence of small divisors. To exemplify, from Eq. (A1) it is easily seen that, in particular cases, the denominator may be vanishingly small. This occurs if $\omega_1 \approx 2\omega_2$, i.e., the frequency of one of the modes of tether transverse vibrations equals half the frequency of a longitudinal mode. From Table 1, it can be seen that this is almost the case of the fundamental longitudinal mode (spring-mass) and the fourth transverse, both of them appearing in the spectra. Similar considerations can be made on the denominators of Eqs. (A2) and (A3). Further, the equivalent formulas of the more complicated third-order solution show that small denominators may occur for a relatively wide variety of relationships between the frequencies of different modes that, therefore, are more likely to reach amplitudes detectable by the accelerometers.

The second feature (common to most nonlinear free vibrations) is the occurrence of combination tones, i.e., of modes with frequencies given by simple combinations of the ones predicted by the linear model. It has already been mentioned in the main text that this characteristic is present in Eqs. (7). To give further examples, let us consider the third-order solution for the longitudinal vibrations; after considerable algebra, it is found that harmonic components may be present with frequencies

$$\omega_1 + 2\omega_2, \qquad \omega_1 - 2\omega_2$$

and the third-order solution for satellite roll/pitch, with the frequencies

$$3\omega_2, \qquad 2\omega_1 + \omega_2, \qquad 2\omega_1 - \omega_2$$

Both of these examples show a plausible explanation for one of the causes why the experimental spectra often contain many more lines than expected by a linear model of tether-satellite vibrations. In fact, it is recalled that ω_1 and ω_2 are the frequencies of any mode of longitudinal and transverse-attitude oscillations. Now, although only the spring-mass mode of the extensional vibrations can be detected by the instruments, several transverse modes are present in many spectra, so that the number of possible combinations is pretty large. Finally, it must be remembered that the SLA is located in a generic point fixed in the satellite, so that the frequencies are further modulated by its attitude motion.

Acknowledgments

This paper presents part of the output of a research program sponsored by Agenzia Spaziale Italiana since 1984. Thanks are due in particular to G. Manarini, Tethered Satellite System Program Manager.

$$C_1 = \frac{S_1 d\Omega_1^2}{\Omega_1^2\left[\Omega_1^2(1 - K_1 d) - K_2(l + d)\right]\sin\lambda + \left[3n^2(l + d)/l\right]\lambda\cos\lambda\left[K_2(l + d) - \Omega_1^2\right]} \qquad \text{(A2)}$$

$$D_1 = \frac{S_1^* d\Omega_1^2\left\{-\sin\lambda/d + \left[3n^2(l + d)\lambda\cos\lambda/ld\Omega_1^2\right]\right\}}{\Omega_1^2\left[\Omega_1^2(1 - K_1 d) - K_2(l + d)\right]\sin\lambda + \left[3n^2(l + d)/l\right]\lambda\cos\lambda\left[K_2(l + d) - \Omega_1^2\right]} \qquad \text{(A3)}$$

References

[1]Bergamaschi, S., Bonon, F., and Legnami, M., "Spectral Analysis of Tethered Satellite System-Mission 1 Vibrations," *Journal of Guidance, Control, and Dynamics,* Vol. 18, No. 3, 1995, pp. 618–624.

[2]Bergamaschi, S., Bonon, F., Merlina, P., and Morana, M., "Theoretical and Experimental Investigation of TSS-1 Dynamics," 44th Congress of the International Astronautical Federation, Paper IAF-93-A.3.21, Graz, Austria, Oct. 1993.

[3]Press, W. H., Teukolsky, S. A., Vetterling, V. T., and Flannery, B. P., *Numerical Recipes in Fortran*, 2nd ed., Cambridge Univ. Press, New York, 1992, Chap. 13.

[4]Bergamaschi, S., Martino, M., Smargiassi, M., Musi, P., Meaney, M., and Steyn, J., "Evaluation of Pre-Deployment Dynamic Noise on TSS-1 During Mission STS-46" AAS/AIAA Astrodynamics Specialist Conf., AAS Paper 93-702, Victoria, BC, Canada, Aug. 1993.

[5]Musi, P., Martino, M., Bergamaschi, S., and Zanetti, P., "Micro-g Noise Measured on Board the Tethered Satellite During the STS-46 Mission," *Proceedings of the International Round Table on Tethers in Space*, European Space Research and Technology Center, Noordwijk, The Netherlands, 1994, pp. 452–463 (ESA WPP-081).

[6]Ferraz-Mello, S., "Estimation of Periods from Unequally Spaced Observations." *Astronomical Journal*, Vol. 86, No. 4, 1981, pp. 619–624.

[7]Tietz, S., "Tether Stiffness Model Modifications Based on Flight Data," Martin Marietta Interoffice Memo, Denver, CO, Feb. 1993.